

High performance color-converted micro-LED displays

Fangwang Gou SID Student Member¹ | En-Lin Hsiang SID Student Member¹ |
Guanjun Tan SID Student Member¹ | Yi-Fen Lan² | Cheng-Yeh Tsai² |
Shin-Tson Wu SID Fellow¹ 

¹College of Optics and Photonics,
University of Central Florida, Orlando,
Florida

²Advanced Technology Research Center,
AU Optronics Corp., Hsinchu, Taiwan

Correspondence

Shin-Tson Wu, College of Optics and
Photonics, University of Central Florida,
Orlando, FL.
Email: swu@ucf.edu

Funding information

a.u.Vista, Inc.

Abstract

A full-color micro-LED display can be achieved by red, green, and blue (RGB) chips or by a blue/ultraviolet (UV) micro-LED array to pump downconverters. The latter helps relieve the burden of epitaxial growth of tri-color micro-LED chips. However, such a color-converted micro-LED system usually suffers from color crosstalk and low efficiency due to limited optical density of color converters. With funnel-tube array and reflective coating on its inner surface, the crosstalk is eliminated, and the optical efficiency can be improved by more than two times. In addition, the ambient contrast ratio is also improved because of higher light intensity. The color gamut of this device is approximately 92% of DCI-P3 standard.

KEYWORDS

ambient contrast ratio, color conversion, color crosstalk, color gamut, micro-LEDs

1 | INTRODUCTION

Micro-LED display is expanding rapidly in recent years because of its outstanding features such as low power consumption, nanosecond response time, long lifetime, high dynamic range, and wide color gamut.^{1–4} However, the high-yield mass transfer process of micro-LEDs from semiconductor wafer to glass substrate remains a challenge.^{5,6} To achieve full-color micro-LED displays, the most commonly used method is to grow red, green, and blue (RGB) micro-LEDs on different wafers, and then assemble them into matrices on the same thin-film transistor (TFT)-based glass substrates through mass-transfer, which requires precise alignment for each pixel. Moreover, the light emission efficiency and degradation rate of RGB micro-LEDs are different; as a result, it may need complicated driving circuit to maintain the color rendering index during operation.

One approach to avoid mass-transfer process is monolithic integration of RGB micro-LEDs via adhesive bonding.⁷ However, the fabrication process is complicated since different semiconductor substrates are required for

growing blue/green micro-LEDs and red micro-LED. Another simpler method utilizes single-color micro-LEDs to excite the color converters, such as phosphors or quantum dots (QDs).^{8–10} For example, UV LED array with pixelated RGB QDs can achieve high efficiency and wide color gamut because no color filter is needed. However, for complete color down-conversion, QDs with a high optical density and a relatively thick layer are required. Therefore, light-recycling components such as distributed Bragg reflector are usually employed to improve the light conversion efficiency, which would degrade the ambient contrast ratio (ACR). To overcome this problem, another solution is to employ blue micro-LEDs to excite color converters in order to obtain white light first, and then utilize color filters to achieve RGB subpixels. In this device configuration, the color down-conversion layer does not need to be pixelated, which is more feasible for manufacturing. However, the color filters would absorb two-thirds of the outgoing light. In addition, color crosstalk would occur due to scattering of the color conversion layer.

In this paper, we propose a funnel-tube array for two-color phosphor-based micro-LED displays in order to

reduce color crosstalk and improve light conversion efficiency simultaneously. Besides, the issue of ambient light reflection from the device is addressed.

2 | DEVICE STRUCTURE

Figure 1A illustrates the device structure of color-converted micro-LED displays (Device 1). It consists of a bottom blue micro-LED array, a layer of two-color (green and red) phosphors as color conversion film, and a top color filter array to form RGB subpixels. The pitch length of the display panel is set to be $150\ \mu\text{m}$, and the color filter size is $L_x = 30\ \mu\text{m}$ and $L_y = 130\ \mu\text{m}$ (Figure 1B). The chip size of blue micro-LED is $W_x = 15\ \mu\text{m}$ and $W_y = 30\ \mu\text{m}$. The system is simulated using ray-tracing software LightTools. For simplicity, we assumed that all the micro-LEDs having the same central wavelength of $448\ \text{nm}$ with Lambertian angular emission distribution. For simulation of the phosphor photoluminescence, their absorption spectrum, color conversion efficiency, and emission spectrum are all taken into account during calculations.^{11,12} The phosphor particle size in the simulation is set to vary from $0.25\ \mu\text{m}$ to $5\ \mu\text{m}$ because of the small pixel size.¹³ And, the thickness of funnel tube was set to be $h = 30\ \mu\text{m}$ according to the optical density of the phosphor. The concentrations of green and red phosphors are adjusted to obtain a white balance for the display system. Compared with QDs, phosphors have the advantages of high thermal stability and resistance to moisture.

In Device 1, when only one pixel emits light and all other pixels are turned off, light leakage may come from the surrounding pixels due to light scattering of the phosphor film, which is referred to as color crosstalk. Figure 2 shows the simulated color image. Although only the RGB subpixels inside the white dashed lines are turned on,

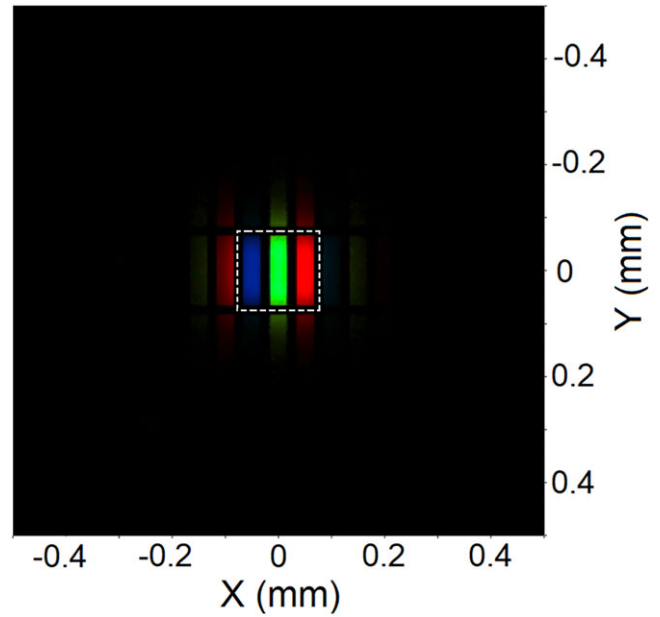


FIGURE 2 Simulated color image of Device 1 when only one pixel inside the white dashed lines is turned on

light leakage outside this region is clearly observed. This problem becomes more severe as the phosphor film gets thicker.^{14,15}

To eliminate color crosstalk, we propose a funnel tube array with taper angles α and β (Device 2) as illustrated in Figure 3A and 3B. It is formed above micro-LED layer while the tube region aligned with each subpixel. The inner surface of the funnel tube can be either absorptive or reflective. The two-color phosphors are filled inside the funnel tube to obtain white light. On top of the funnel-tube array, the color filters with RGB subpixels are aligned with each tube region. In the system, the phosphors for each subpixel region are designed to be totally isolated. Thus, the color crosstalk will be eliminated. Figure 4 shows the simulated color image of

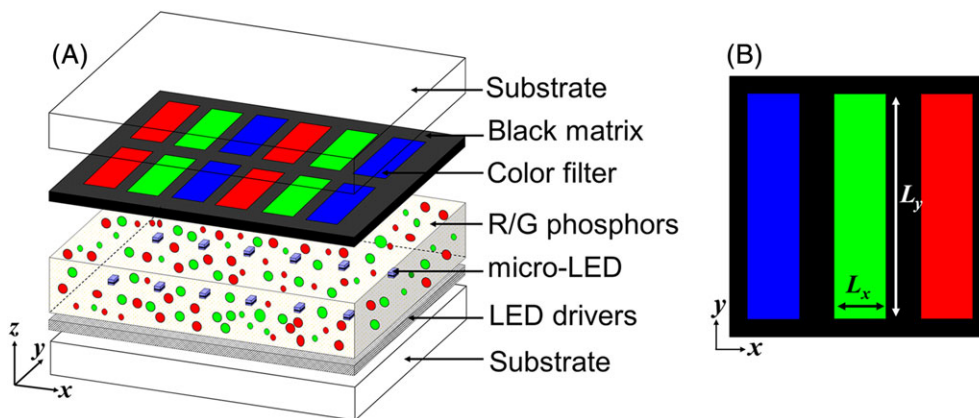


FIGURE 1 A, Schematic diagram for configuration of full color micro-LED display (Device 1). B, Top view of one pixel. $L_x = 30\ \mu\text{m}$, $L_y = 130\ \mu\text{m}$

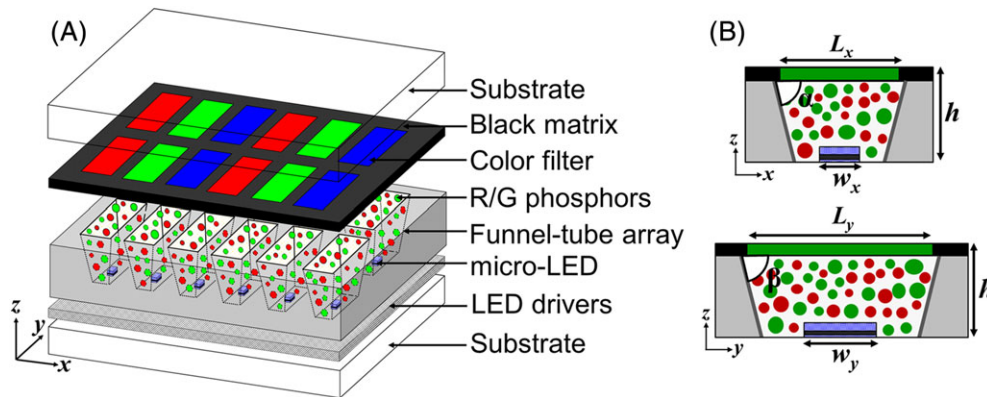


FIGURE 3 A, Schematic diagram for configuration of full color micro-LED display with funnel-tube array (Device 2). B, Cross-sectional views of Device 2. $L_x = 30 \mu\text{m}$, $L_y = 130 \mu\text{m}$, $W_x = 15 \mu\text{m}$, $W_y = 30 \mu\text{m}$, and $h = 30 \mu\text{m}$. The taper angles in x - z plane and y - z plane are α and β , respectively

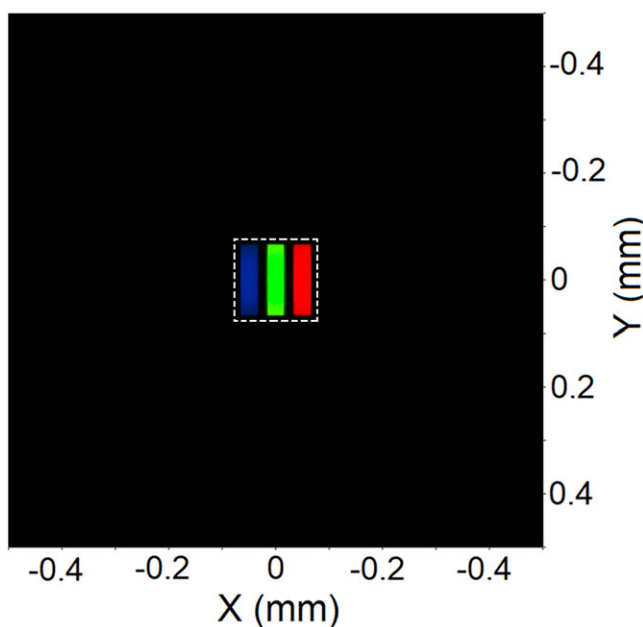


FIGURE 4 Simulated color image of Device 2 when only one pixel that inside the white dashed line is turned on

Device 2. As can be seen, there is no light leakage outside the turned-on pixel region.

3 | SIMULATED RESULTS AND DISCUSSIONS

3.1 | Color gamut

Vivid color is a key metric for display devices, as it enables a more realistic viewing experience. Generally, light sources with a narrower full width at half maximum (FWHM) would lead to a wider color gamut.¹⁶ In our modeling, we use a combination of green phosphor (β -sialon: Eu²⁺, FWHM ~ 50 nm) and red phosphor

(CaAlSiN₃:Eu²⁺)¹⁷ to improve the color performance. Figure 5 depicts the spectrum of blue micro-LED pumped the two-color phosphors and the simulated color gamut in CIE 1931 color space is shown in Figure 6. This system covers 92% of DCI-P3 standard¹⁸ and 67% of Rec. 2020 standard.^{19,20} Alternative color converters such as CdSe red/green QDs with FWHM approximately 25-30 nm can also be used to obtain wider color gamut.^{21,22} However, the device structure, especially the thickness of the funnel-tube array, needs to be optimized according to the optical density of the color converters.

3.2 | Light efficiency

In order to eliminate the color crosstalk, the phosphors for each subpixel should be optically isolated by depositing absorptive or reflective coatings on the inner side surface

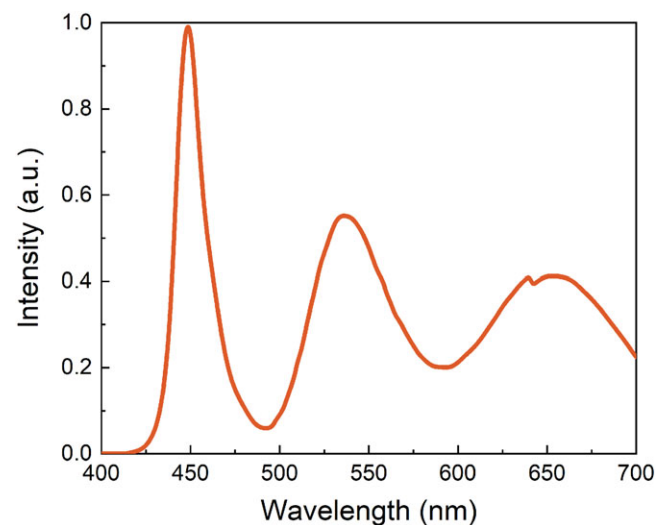


FIGURE 5 Simulated spectrum of Device 2 when all of the pixels are turned on

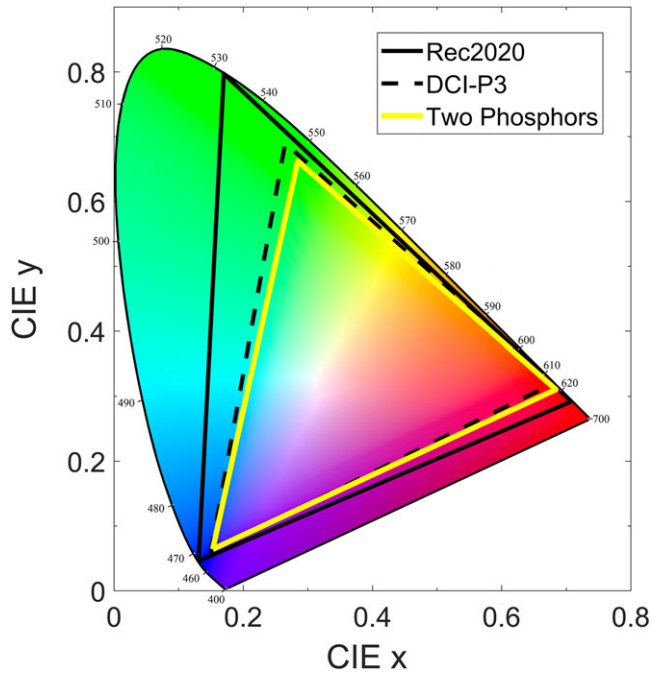


FIGURE 6 Simulated color gamut for Device 2 with red/green phosphor in CIE 1931 color space

of funnel tube. Furthermore, the taper angles (α and β) of the funnel tube need to be optimized for improvement of the light efficiency. The simulated relative light intensities of Device 2 with absorptive and reflective coatings normalized to that of Device 1 are plotted in Figure 7A and 7B. Specifically, in Figure 7A, the taper angle α varied from 76° to 108° , while α was fixed at 80° ; in Figure 7B, the taper angle β varied from 31° to 108° when α was set to be 80° . For absorptive coating, the light intensity slightly increased as taper angle increased because more forward emission was absorbed. The relative intensity is as low as 0.62 even for $\alpha = 108^\circ$ and $\beta = 80^\circ$. As a comparison, the light intensity for reflective coating is more than three times higher than that of absorptive one since the inner reflector could recycle light and elongate the effective optical path inside the phosphors. The light intensity decreased as the taper angle increased. When the taper angle was larger than 90° , more light was reflected downwards by the inner reflector and then absorbed or scattered by the backplane. On the other hand, when the taper angle was less than 90° , more light was reflected upwards, which then escaped from the device to the air. Therefore, a taper angle less than 90° was preferred to obtain higher light efficiency.

3.3 | Luminous ambient light reflectance

In addition to light emission intensity, luminous ambient light reflectance also needs to be investigated because it

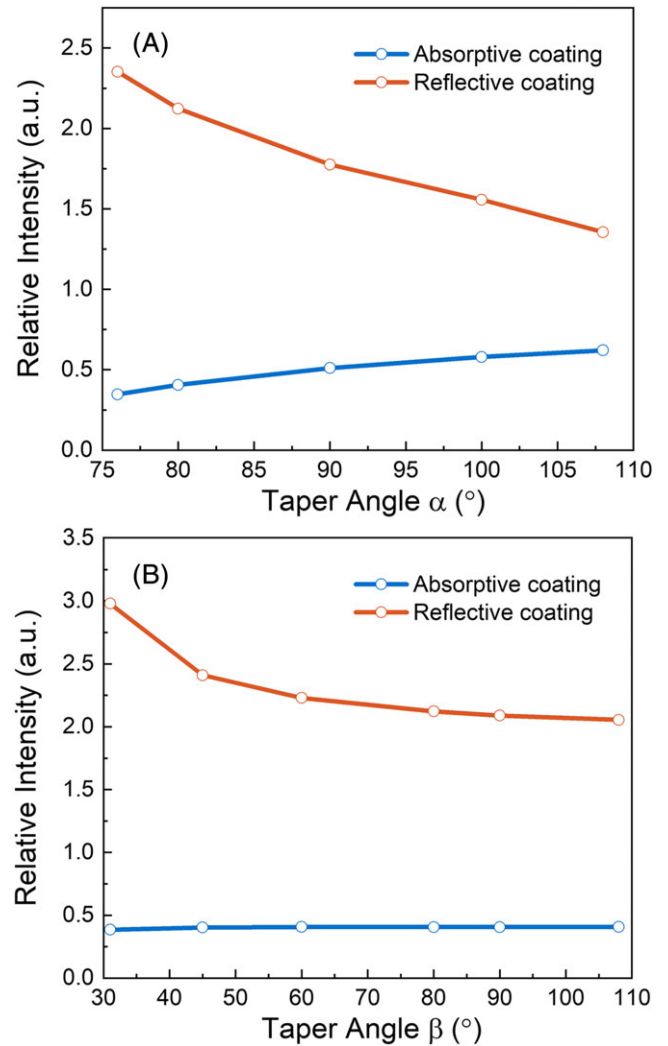


FIGURE 7 Relative light intensity of Device 2 with absorptive coating and reflective coating as a function of taper angle A, α when $\beta = 80^\circ$, and B, β when $\alpha = 80^\circ$. The light intensity is normalized to that of Device 1

determines a display's performance in the presence of ambient light, which is referred as ACR. Luminous ambient light reflectance can be defined as²³

$$R_L = \frac{\int_{\lambda_1}^{\lambda_2} V(\lambda)S(\lambda)R(\lambda)d\lambda}{\int_{\lambda_1}^{\lambda_2} V(\lambda)S(\lambda)d\lambda}, \quad (1)$$

In Equation 1, $V(\lambda)$ is the photopic human eye sensitivity function, $R(\lambda)$ is the spectral reflectance of the display device, and $S(\lambda)$ is the spectrum of ambient light. In our modeling, we used CIE standard D65 as light source.

Figure 8A and 8B show the calculated luminous ambient light reflectance of Device 2 with absorptive coating and reflective coating as a function of taper angle. The

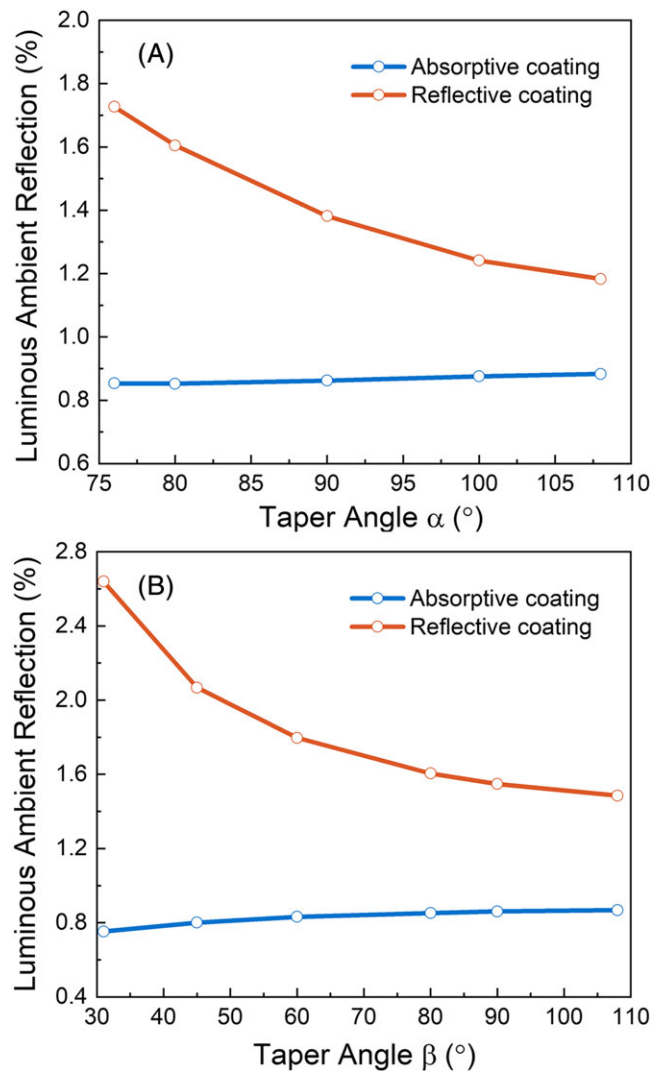


FIGURE 8 Luminous ambient light reflectance of Device 2 with absorptive coating and reflective coating as a function of taper angle A, α when $\beta = 80^{\circ}$, and B, β when $\alpha = 80^{\circ}$

trend is similar to that of light intensity, indicating that higher intensity associated with higher ambient light reflectance. For funnel-tube absorptive coating, the ambient reflectance is approximately 0.8, which is much smaller than that of reflective coating (1.2~2.6).

In order to further understand the ambient light reflection, we plot the reflectance for RGB subpixels of structure with reflective coating and $\alpha = 80^{\circ}$ and $\beta = 80^{\circ}$ as well as transmittance of color filters in Figure 9. The reflectance spectral profiles are very similar to the transmittance of color filters except for the lower intensity of the blue light. For the blue subpixel, the blue component of the ambient light transmitted through the color filter and entered the funnel tube, some of the light were absorbed and then converted by the phosphor, and other light was scattered and reflected inside the funnel tube. A part of the unconverted blue light could escape from the

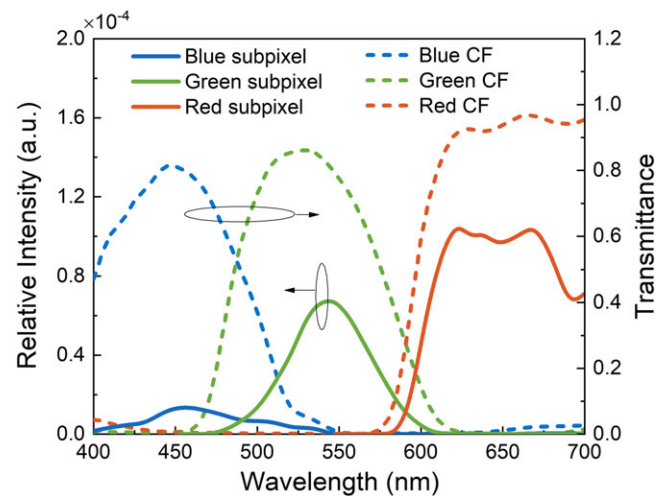


FIGURE 9 Ambient light reflectance (solid lines, left y axis) for red, green, and blue (RGB) subpixels of Device 2 with reflective coating and taper angle $\alpha = 80^{\circ}$ and $\beta = 80^{\circ}$, and transmittance of RGB color filters (dashed lines, right y axis)

color filter. For green and red subpixels, the ambient light was scattered by the phosphor particles or reflected by the funnel tube back to the air, leading to higher reflectance. Table 1 lists the luminous ambient light reflectance for each subpixel of structure with reflective coating and $\alpha = 80^{\circ}$ and $\beta = 80^{\circ}$. Because of human eye sensitivity, ambient reflection from green subpixel was dominant.

3.4 | Ambient contrast ratio

The ACR of these three structures was calculated using the following equation^{23–25}:

$$ACR = \frac{L_{on} + L_{ambient} \cdot R_L}{L_{off} + L_{ambient} \cdot R_L} \quad (2)$$

In Equation 2, L_{on} (L_{off}) is the on-state (off-state) luminance value of a display, $L_{ambient}$ represents the ambient luminance, and R_L is the luminous reflectance of the display panel. To calculate ACR, we assumed L_{on} of Device 1 (without funnel tube) to be 1000 nits, while L_{on} of Device 2 with absorptive and reflective coating and taper angle of $\alpha = 80^{\circ}$ and $\beta = 80^{\circ}$ can be calculated according to the relative intensity, the results are 405 nits and 2123 nits,

TABLE 1 Luminous ambient reflectance for RGB subpixels of Device 2 with reflective coating and taper angle $\alpha = 80^{\circ}$ and $\beta = 80^{\circ}$

Pixels	RGB	Blue	Green	Red
Luminous reflectance	1.61%	0.05%	1.02%	0.54%

Abbreviation: RGB, red, green, and blue.

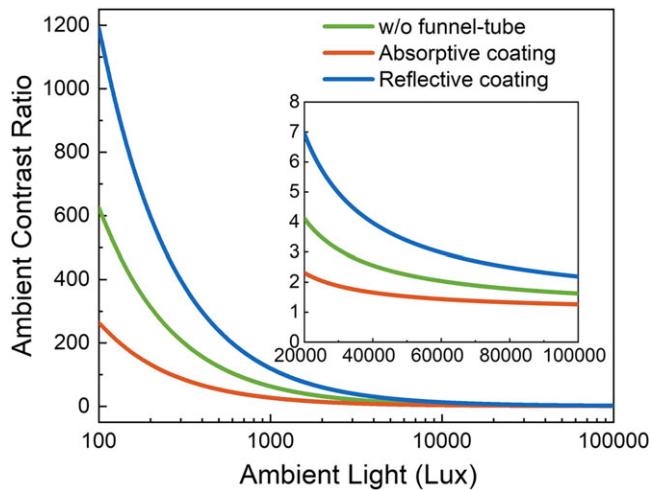


FIGURE 10 Simulated ambient contrast ratio of Device 1 and Device 2 with absorptive coating and reflective coating on the side inner surface of funnel tube. Taper angle $\alpha = 80^\circ$ and $\beta = 80^\circ$. The top surface reflectance is 4% without antireflection (AR) coating

respectively. As an emissive-type display, L_{off} of micro-LED is 0. The surface reflectance was assumed to be 4%. The calculated ACR is depicted in Figure 10. As ambient illumination got stronger, the ACR decreased dramatically first and gradually saturated. Although funnel tube with reflective coating had the most severe ambient reflection, it achieved the largest ACR under different ambient light conditions because of its highest brightness. Under strong ambient light conditions such as full daylight ($\sim 20\,000$ lux), the ACR of Device 1 and Device 2 with absorptive coating were all less than 5:1 (inset of

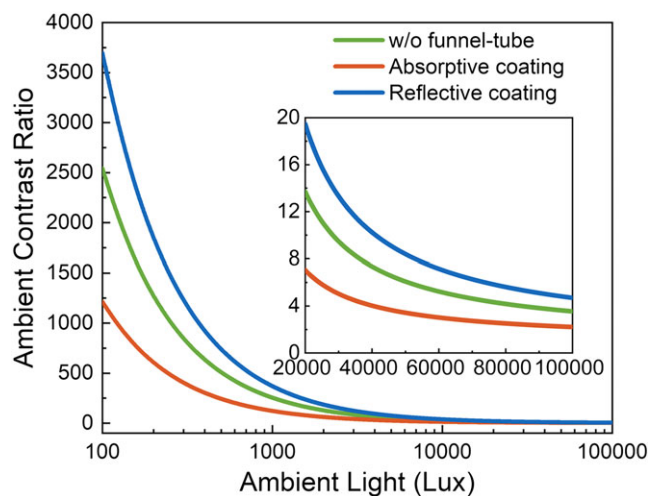


FIGURE 11 Simulated ambient contrast ratio of Device 1 and Device 2 with absorptive coating and reflective coating on the side inner surface of funnel tube. Taper angle $\alpha = 80^\circ$ and $\beta = 80^\circ$. The top surface reflectance is 0.2% with antireflection (AR) coating

Figure 10), which is barely readable under sunlight.²⁶ This relatively low ACR originates from both light scattering by the phosphor particles and surface reflection. To improve ACR, antireflection (AR) coating with a surface reflectance of about 0.2% could be employed²⁷; results are shown in Figure 11. When $L_{\text{ambient}} = 20\,000$ lux, the ACR of Device 2 with absorptive coating could be improved to approximately 7:1, which is adequately readable in sunlight. While for Device 2 with reflective coating, the ACR is approximately 20:1, indicating an excellent readability.

4 | CONCLUSION

In this work, we proposed a funnel-tube array to eliminate the color crosstalk of the color-converted micro-LED displays. With reflective coating on the inner side surface of the funnel-tube and taper angle of 80° , the light efficiency of the device could be increased by more than approximately two times. Moreover, the ACR was also improved due to higher light intensity, despite the increased ambient reflectance. By utilizing two-color phosphors, which have high thermal stability and resistance to moisture, the color gamut of this device covers 92% of DCI-P3 standard.

ACKNOWLEDGMENT

The authors are indebted to a.u.Vista, Inc. for the financial support.

ORCID

Shin-Tson Wu  <https://orcid.org/0000-0002-0943-0440>

REFERENCES

- Jin SX, Li J, Li JZ, Lin JY, Jiang HX. GaN microdisk light emitting diodes. *Appl Phys Lett*. 2000;76(5):631–633. <https://doi.org/10.1063/1.125841>
- Jiang HX, Lin JY. Nitride micro-LEDs and beyond—a decade progress review. *Opt Express*. 2013;21(S3):A475–A484. <https://doi.org/10.1364/OE.21.00A475>
- Liu Z, Chong WC, Wong KM, Lau KM. GaN-based LED microdisplays for wearable applications. *Microelectron Eng*. 2015; 148:98–103. <https://doi.org/10.1016/j.mee.2015.09.007>
- Huang Y, Tan G, Gou F, Li M-C, Lee S-L, Wu S-T. Prospects and challenges of mini-LED and micro-LED displays. *J Soc Inf Display*. 2019. In press. <https://doi.org/10.1002/jsid.760>
- Virey EH, Baron N. Status and prospects of microLED displays. *SID Int Symp Digest Tech Papers*. 2018;49(1):593–596. <https://doi.org/10.1002/sdtp.12415>

6. Paranjpe A, Montgomery J, Lee SM, Morath C. Micro-LED displays: key manufacturing challenges and solutions. *SID Int Symp Digest Tech Papers*. 2018;49(1):597–600. <https://doi.org/10.1002/sdtp.12414>
7. Kang CM, Lee JY, Kong DJ, et al. Hybrid full-color inorganic light-emitting diodes integrated on a single wafer using selective area growth and adhesive bonding. *ACS Photonics*. 2018;5(11):4413–4422. <https://doi.org/10.1021/acsp Photonics.8b00876>
8. Han HV, Lin HY, Lin CC, et al. Resonant-enhanced full color emission of quantum-dot-based micro-LED display technology. *Opt Express*. 2015;23(25):32504–32515. <https://doi.org/10.1364/OE.23.032504>
9. Lin HY, Sher CW, Hsieh DH, et al. Optical cross-talk reduction in a quantum-dot-based full-color micro-light-emitting-diode display by a lithographic-fabricated photoresist mold. *Photon Res*. 2017;5(5):411–416. <https://doi.org/10.1364/PRJ.5.000411>
10. Chen GS, Wei BY, Lee CT, Lee HY. Monolithic red/green/blue micro-LEDs with HBR and DBR structures. *IEEE Photonics Technol Lett*. 2018;30(3):262–265. <https://doi.org/10.1109/LPT.2017.2786737>
11. Zollers M. Phosphor modeling in LightTools, LightTools White Paper 2011. <http://optics.synopsys.com/lighttools/pdfs/ModelingPhosphorsInLightTools.pdf>.
12. Tran NT, You JP, Shi FG. Effect of phosphor particle size on luminous efficacy of phosphor-converted white LED. *J Lightwave Technol*. 2009;27(22):5145–5150. <https://doi.org/10.1109/JLT.2009.2028087>
13. Fern GR, Harris PG, Ireland TG, Silver J. Sub-micrometre phosphor preparation for next generation displays. *SID Int Symp Digest Tech Papers*. 2017;48(1):1711–1714. <https://doi.org/10.1002/sdtp.11996>
14. Silver J, Harris P, Fern G, Bonar J, Valentine G, Gorton S. A novel approach to the manufacture of microLED colour conversion structures *International Displays Workshop*, Fukuoka, Japan, 7-9th December 2016. <http://bura.brunel.ac.uk/handle/2438/13965>.
15. Gou F, Hsiang EL, Tan G, Lan YF, Tsai CY, Wu ST. Tripling the optical efficiency of color-converted micro-LED displays with funnel-tube array. *Crystals*. 2019;9(1):39. <https://doi.org/10.3390/cryst9010039>
16. Chen H, He J, Wu ST. Recent advances on quantum-dot-enhanced liquid-crystal displays. *IEEE J Sel Top Quantum Electron*. 2017. <https://doi.org/10.1109/JSTQE.2017.2649466>; 23(5):1–11.
17. Wang L, Wang X, Kohsei T, et al. Highly efficient narrowband green and red phosphors enabling wider color-gamut LED backlight for more brilliant displays. *Opt Express*. 2015;23(22):28707–28717. <https://doi.org/10.1364/OE.23.028707>
18. SMPTE RP 431–2:2011 D-cinema quality—reference projector and environment. 2011
19. Recommendation ITU-R BT.2020 Parameter values for ultra-high definition television systems for production and international programme exchange, 2012.
20. Masaoka K, Nishida Y, Sugawara M, Nakasu E. Design of primaries for a wide-gamut television colorimetry. *IEEE Trans Broadcast*. 2010;56(4):452–457. <https://doi.org/10.1109/TBC.2010.2074450>
21. Zhu R, Luo Z, Chen H, Dong Y, Wu ST. Realizing Rec. 2020 color gamut with quantum dot displays. *Opt Express*. 2015;23(18):23680–23693. <https://doi.org/10.1364/OE.23.023680>
22. Chen H, Zhu R, He J, et al. Going beyond the limit of an LCD's color gamut. *Light: Sci Appl*. 2017;6:e17043. <https://doi.org/10.1038/lsa.2017.43>
23. Singh R, Unni KN, Solanki A. Improving the contrast ratio of OLED displays: an analysis of various techniques. *Opt Mater*. 2012;34(4):716–723. <https://doi.org/10.1016/j.optmat.2011.10.005>
24. Dobrowolski JA, Sullivan BT, Bajcar RC. Optical interference, contrast-enhanced electroluminescent device. *Appl Optics*. 1992;31(28):5988–5996. <https://doi.org/10.1364/AO.31.005988>
25. Chen H, Tan G, Wu ST. Ambient contrast ratio of LCDs and OLED displays. *Opt Express*. 2017;25(26):33643–33656. <https://doi.org/10.1364/OE.25.033643>
26. Walker G. GD-Itronix Dynavue Technology. The ultimate outdoor-readable touch-screen display (Rugged PC Review, 2007). http://www.ruggedpcreview.com/3_technology_itronix_dynavue.html.
27. Tan G, Lee JH, Lan YH, et al. Broadband antireflection film with moth-eye-like structure for flexible display applications. *Optica*. 2017;4(7):678–683. <https://doi.org/10.1364/OPTICA.4.000678>

AUTHOR BIOGRAPHIES



Fangwang Gou received her Bachelor of Science (BS) degree from the University of Electronic and Science and Technology of China in 2012 and Master of Science (MS) degree from Peking University, China, in 2015. Currently, she is working toward the Doctor of Philosophy (PhD) degree at the College of Optics and Photonics, University of Central Florida, USA. Her research focuses on display optics for liquid crystals, virtual reality (VR)/augmented reality (AR), and micro-LEDs. She received SID Distinguished Student Paper Awards in 2016 and 2018.

En-Lin Hsiang received his BS degree from National Chiao Tung University, Hsinchu, Taiwan in 2014 and MS degree from National Chiao Tung University, Hsinchu, Taiwan, in 2016. Currently, he is working toward the PhD degree at College of Optics and Photonics, University of Central Florida, USA. His current research focuses on micro-LED and mini-LED display.

Guanjun Tan received a BS degree in Physics from University of Science and Technology of China in

2014, and is currently working toward the PhD degree at the College of Optics and Photonics, University of Central Florida. His current research interests include head-mounted display, organic LED display, and novel liquid crystal display technologies.

Yi-Fen Lan received his PhD degree from National Taiwan University in 2010. Currently, he is a principal engineer at AU Optronics Corporation.

Cheng-Yeh Tsai received the MS degree in Electrical-Optical engineering from National Taiwan University, Taiwan, in 2003. Currently, he is a senior manager at AU Optronics Corporation.



Shin-Tson Wu is Pegasus professor at the College of Optics and Photonics, University of Central Florida. He is among the first six inductees of the Florida Inventors Hall of Fame (2014) and a Charter Fellow of the National Academy of Inventors (2012). He is a Fellow of the IEEE, OSA, SID, and SPIE, and an honorary professor of Nanjing University

(2013) and of National Chiao Tung University (2017). He is the recipient of 2014 OSA Esther Hoffman Beller Medal, 2011 SID Slottow-Owaki Prize, 2010 OSA Joseph Fraunhofer Award, 2008 SPIE G. G. Stokes Award, and 2008 SID Jan Rajchman Prize. Presently, he is serving as SID honors and awards committee chair.

How to cite this article: Gou F, Hsiang E-L, Tan G, Lan Y-F, Tsai C-Y, Wu S-T. High performance color-converted micro-LED displays. *J Soc Inf Display*. 2019;27:199–206. <https://doi.org/10.1002/jsid.764>